LEGIBILITY NOTICE

A major purpose of the Technical Information Center is to provide the broadest dissemination possible of information contained in DOE's Research and Development Reports to business, industry, the academic community, and federal, state and local governments.

Although a small portion of this report is not reproducible, it is being made available to expedite the availability of information on the research discussed herein.

1

LA-UR -83-258

Conf - 821159 - -2

LA-UR--83-258

DE83 006077

TITLE: SOLAR WIND IRON ABUNDANCE VARIATIONS AT SOLAR WIND SPEEDS > 600 km s^{-1}, 1972-1976

AUTHOR(S): D.G. Mitchell, E.C. Roelof and S.J. Bame

SUBMITTED TO: Solar Wind 5 Conference proceedings
Woodstock, Vermont, November 1-5, 1982

Los Alamos National Laboratory
Los Alamos, New Mexico 87545

SOLAR WIND IRON ABUNDANCE VARIATIONS AT SOLAR WIND SPEEDS > 600 km s^{-1}, 1972-1976

D. G. Mitchell[1], E. C. Roelof[1] and S. J. Bame[2]

[1]Applied Physics Laboratory
Johns Hopkins University
Laurel, Maryland 20707

[2]Los Alamos National Laboratory
Los Alamos, New Mexico 87545

Submitted to Proceedings, Solar Wind 5

JANUARY 1983

ABSTRACT

We have analyzed the Fe/H ratios in the peaks of high speed streams (HSS) during the decline of Solar Cycle 20 and the following minimum (October 1972-December 1976). We utilized the response of the 50-200 keV ion channel of the APL/JHU energetic particle experiment (EPE) on IMP-7 and 8 to solar wind iron ions at high solar wind speeds ($V \gtrsim 600$ km sec^{-1}), and compared our Fe measurements with solar wind H and He parameters from the Los Alamos National Laboratory (LANL) instruments on the same spacecraft. In general, the Fe distribution parameters (bulk velocity, flow direction, temperature) are found to be similar to the LANL He parameters. Although the average Fe/H ratio in many steady HSS peaks agrees within observational uncertainties with the nominal coronal ratio of 4.7×10^{-5}, abundance variations of a factor of up to 6 are obtained across a given coronal-hole associated HSS. There are, as well, factor of 2 variations between stream-averaged abundances for recurrent HSS emanating from different coronal holes occurring on the sun on the same solar rotation. Flare-related solar wind streams sometimes show Fe/H ratios enhanced by factors of 4-5 over coronal-hole associated, quiet time streams. Over the period 1973-1976, a steady decrease in the average quiet-time Fe/H ratio by a factor ~ 4 is measured on both IMP-7 and 8.

INTRODUCTION

The literature on solar wind iron ions in the peaks of high speed streams (HSS) is characterized by a paucity of direct measurements combined with a fairly well developed theoretical framework based on inference from related data.

Contemporary plasma detectors (electrostatic analyzers and mass spectrometers) are limited in measuring iron ions at high solar wind speeds (> 600 km sec^{-1}) with their attendant high kinetic temperatures. An alternate, though unexpected, technique has been shown in Mitchell and Roelof (1980) and Mitchell et al. (1981a) to be capable of high time resolution measurements of solar wind iron under precisely these conditions. The technique uses the 50 - 200 keV ion channel of the Energetic Particle Experiments (EPE), D. J. Williams, Principal Investigator, on the IMP 7/8 spacecraft. Another measurement of iron in high speed solar wind, including charge state determination, was reported by Ipavich et al. (1983) who also employed a solid state detection system. In Mitchell et al. (1981a), we showed that under favorable conditions we could use the EPE data in conjunction with solar wind hydrogen and helium data (from the Los Alamos National Laboratories Plasma Analyzers on IMP-7 and 8, S. J. Bame, Principal Investigator) to determine the iron bulk velocity, temperature, and abundance. These quantities were then related to the hydrogen and helium distribution parameters. The bulk velocity and temperature of the Fe were found to agree qualitatively with measurements made at lower velocities of other minor ions: He, as discussed in Neugebauer (1981), Ogilvie (1975), Asbridge et al. (1976), Hirshberg et al. (1974), Marsch et al. (1982a), and many others; O, Fe and other minor ions as discussed in Ogilvie (1980), Hollweg and Turner (1978), Dusenbury and Hollweg

(1981), Isenberg and Hollweg (1982), Marsch et al. (1982b), and references therein. In addition, abundances were found to be nearly coronal (as expected) see, for example, Geiss and Bochsler (1981) who suggested some Fe enhancement associated with solar flare activity, similar to results given in Bame (1981).

In all the literature cited, however, there are very few actual measurements of solar wind iron, and none at high solar wind velocities (> 600 km sec^{-1}), save those in Mitchell and Roelof (1980) and Mitchell et al. (1981a). In addition to being able to measure iron at high bulk velocities in the first place, the uniqueness of the observations presented here lies in their continuity over periods on scales of hours, days, or years so that we can investigate variations in abundance and other distribution function parameters in individual streams, and even the evolution of streams themselves over the decline of the last solar cycle.

TECHNIQUE

The data analyzed in this work were obtained using the 50 - 200 keV ion channel of the Johns Hopkins Applied Physics Laboratory Energetic Particle Experiment on the IMP-7 and 8 spacecraft. This channel (L1) employs a silicon surface barrier solid state detector coated with 40 $\mu g\text{-}cm^{-2}$ of aluminum and with an electronic threshold of 30 keV, mounted in a telescope spinning with the spacecraft with a 15° opening angle and sectored into 16 sectors in the ecliptic plane. Iron ions in the high speed solar wind have sufficient energy due to their bulk velocity to trigger the detector with an efficiency which is a strong function of velocity. A complete description of the instrument can be found in Williams (1977) and detailed discussions of the L1 channel

response to the iron ions are contained in Mitchell and Roelof (1980) and Mitchell et al. (1981a), hereafter referred to as Paper 1 and Paper 2.

As described in Papers 1 and 2, the iron is seen primarily in Sectors 9 and 10, the sunward-looking sectors. The ratio of Sector 9 to Sector 10 is a sensitive function of the iron east-west bulk flow angle. In Paper 2, we describe in detail a method whereby for certain events we can derive both the iron bulk flow velocity (V_{Fe}) and its thermal velocity (v_{Fe}), assuming a convected Maxwellian thermal iron distribution. Using the model from Paper 2 for the instrument response based upon detector calibrations and geometry, we can use the measured V_{Fe} and v_{Fe} to obtain the iron flux, $J_{Fe} = N_{Fe} V_{Fe}$. This work will concern itself primarily with the quantity $J_{Fe}/J_H = N_{Fe} V_{Fe}/N_H V_H$ N_{Fe}/N_H, the iron abundance relative to hydrogen in the solar wind. We shall use the notation Fe/H for this abundance ratio through the remainder of this paper.

It has been shown (Ogilvie, 1980; Bochsler and Geiss, 1982) that minor ions up to oxygen, and perhaps iron, behave similarly to each other (same bulk velocity and thermal velocity) but dissimilarly to hydrogen (different, usually higher bulk velocity) in the non-collisional solar wind. In Figure 1a, we plot 5.5 minute averages of the sum of the count-rates in Sectors 9 and 10 on IMP-7 normalized by hydrogen flux, versus the hydrogen bulk velocity from the Los Alamos National Laboratory (LANL) solar wind detector on IMP-7. In Figure 1b we plot the sum of Sectors 9 and 10 normalized by the LANL helium flux, versus the LANL helium velocity. It can readily be seen that V_{He} orders the data much better than V_H, in agreement with $V_{He} \approx V_{Fe} \neq V_H$. Throughout the remainder of this paper, we assume $V_{Fe} = V_{He}$ and use V_{He} to remove the detector efficiency velocity dependence.

Although the model for the detector response includes the detector geometry, V_{Fe}, and v_{Fe}, it is dominated by V_{Fe} alone. Using plots such as that in Figure 1b for individual high speed streams, we have found empirically that the instrument response velocity dependence is well approximated by ${V_{Fe}}^{13}$. However, we know that $V_{Fe} \approx V_{He}$, so if we multiply the measured fluxes by ${V_{He}}^{-13}$ and use the model calculation to determine the proper normalization, we obtain a very good approximation to N_{Fe} V_{Fe} model which takes much less computer time to run.

In Figure 2 we demonstrate the application of this technique with a high speed stream (an occurrence of the "monster" stream) from day 54 - 60, 1973 with solar wind parameters measured using the LANL instrument on IMP-7. In the top panel, we plot V_H (solid line) and V_{He} (dots). The third panel is v_H parallel and v_H perpendicular to the heat flux direction (which is close to the IMF) connected by a vertical bar. Also appearing here in dots is v_{He}, offset downward by 25 km s^{-1} so that it is not obscured by v_H. In the fourth panel, we plot the hydrogen density (N_H, solid line) and the He/H ratio (dots, separate scale) on log scales.

The second panel displays Fe/H normalized by the coronal value of 4.7×10^{-5} of Withbroe (1971), which is also nearly the same as the solar wind value of 5.3×10^{-5} obtained (at lower solar wind velocity and kinetic temperature than those at which we are working) by Bame et al. (1979) for inter-stream solar wind. The absolute normalization of Fe/H is not well determined; flight spare detectors were used in the detector calibrations, and though there is good qualitative agreement between IMP-7, IMP-8, and the spare detectors, when simultaneously sampling data from a particular stream IMP-7 and 8 disagree with one another by a factor of $\sim$ 3 in absolute response. On

the basis of that consistent pattern, we have removed that factor of 3 difference in this paper, multiplying all IMP-7 data by 3 before plotting. The model calculates the absolute Fe/H value based upon the instrument response, assuming the flight detectors have the same absolute response as the spare detectors used in the accelerator calibrations described in Paper 1. Since the two flight detectors disagree by a factor of 3, we expect the offset error in our absolute Fe/H values to be at least that large. The data are plotted assuming that IMP-8 responded absolutely as one of the calibrated spares (because it gives Fe/H ratios closer to the nominal coronal abundances), and we normalize all the data (IMP-8 and 3 × IMP-7) by the nominal coronal value.

The relative variations of Fe/H are much better determined. Errors enter mainly from the following sources: 1) errors in the determination of V_{He} and the deviation of $V_{Fe} - V_{He}$ from zero; 2) v_{Fe} may not be precisely equal to v_{He}; 3) poor counting statistics for iron at solar wind velocities $\lesssim$ 650 km s^{-1}; 4) flow angles more than ~ 5 degrees out of the ecliptic; 5) sensitivity to soft solar x-rays; 6) high background level due to energetic proton and/or alpha particle events.

In Figure 2, the random errors in the hourly averages of the iron abundance are estimated to be very small. The statistically significant variation on a time scale of a fraction of a day is in fact not random; individual hourly values are clearly not independent but quite correlated with the previous and succeeding hours. Furthermore, though it is impossible to discern in this format, the Fe and He abundance ratios are at times highly correlated on a fraction of a day time scale, although they are not well correlated on the scale of the stream width, i.e. several days. Systematic

errors, as stated earlier, may render the absolute abundance values uncertain; however, the errors in the relative abundances should remain low as long as the six major sources of error mentioned above do not enter significantly. From the scatter in Figure 1b, one can see that this is generally the case for $V_{He} \gtrsim 660$ km s^{-1}.

IRON ABUNDANCE AS A FUNCTION OF HELIOGRAPHIC SOURCE LONGITUDE

Using the technique discussed in the previous section, we can obtain reliable estimates of Fe/H as a function of time throughout most periods of high velocity solar wind flow. Beginning in 1977, the increase in quiescent solar soft x-ray flux (to which channel L1 also responds) associated with the rise of the solar cycle produces too high a background to use this technique. Therefore, we shall concentrate our analysis on the period from the launch of IMP-7 (day 270, 1972) to the end of 1976, which coincides with the period of long-lasting, corotating, coronal hole-associated high speed solar wind streams. Since we are interested in the coronal source regions and their influence on Fe/H, we wish to examine the variation of Fe/H as a function of the heliographic location of its source in the corona. To this end we shall map the time-ordered data into heliographic source longitude, using the constant radial velocity approximation from the corona to 1 AU.

We are working initially with 5.5 minute averages of the iron and solar wind data, which we map into 2° longitude bins and average all 5.5 minute points which map into the same longitude bin. Since the sub-terrestrial heliographic longitude changes at a rate of ~ 13.3°/day, a 2° bin corresponds nominally to ~ 3.1 hours of data for periods of roughly constant velocity. During the rise of streams, the source longitude changes quickly

with increasing velocity resulting in many fewer points per 2° bin and correspondingly higher statistical uncertainty. The rise also is an interaction region including solar wind from many longitudes and therefore a non-unique source longitude. In the decay of streams, the source longitude can remain roughly constant for up to two days, resulting in bin averages made up of many data points associated with a broad range of source region velocities, with the lower velocities contributing disproportionately to the errors due to Points 3 and 5 discussed above. Therefore, we will direct our attention to periods when the velocity is constant or changing relatively slowly.

The data from the upper two panels of Figure 2 are mapped back to their source longitude in the light lines in Figure 3, as an example of this technique. Nothing has really changed in the stream maximums, except there is less temporal resolution and time does not appear explicitly (implicitly, time increases non-uniformly from right to left in this format). This particular stream maps to a longitude range spanning nearly 90° of the corona, and has been associated by Nolte et al. (1976) and Hundhausen (1977) with the equatorward extension of the south polar coronal hole. In this case, Fe/H is roughly constant over a coronal source region which subtends one quarter of the solar circumference. To investigate the longer term stability of this structure, we compare, in Figure 3, the same stream with its recurrence on the following solar rotation (heavy lines). Although the stream's leading edge has moved westward approximately 40°, the average value of Fe/H has not changed significantly, and, in fact, can be considered a stable signature of this source region. This stream is unusual in its breadth and the good coverage by IMP-7 on consecutive rotations, but the repeatability of the Fe/H profile is a common feature of other stable corotating streams associated with coronal holes.

A particularly striking example of the similarity between the behavior of the He and Fe bulk flows can be seen in Figure 4. This stream (days 116 - 123, 1973) seen on IMP-7 was shortlived, appearing on the previous rotation as a smaller stream with a peak near 600 km s^{-1} and on the following rotation even smaller with a peak of ~ 475 km s^{-1}. On this rotation, the stream is preceded and accompanied by a number of energetic particle-producing flares up to 2B in importance. Thus the stream is probably flare-related and not corotating, and the very high Fe/H recorded may be typical of flare-associated blasts of solar wind. High Fe/H associated with flare activity was also observed on days 188 - 191, 1974 and an enhancement persisted at the active longitude on the following rotation, after the flare activity had ceased. Because this is a flare-associated stream, the interplanetary dynamics differ from those of corotating streams, and, in particular, in the bottom panel, lower curve, we measure abnormally large deviations from 0° in the east-west flow angle ϕ_{He}. The upper curve in the lower panel of Figure 4 is a plot of the logarithm of the Sector 10 to Sector 9 ratio. Simulations using our model lead us to expect that we should observe a logarithmic relationship between the iron east-west angle ϕ_{Fe} and the ratio of fluxes in Sectors 10 and 9, $\phi_{Fe} \propto \log (10/9)$, assuming that V_{Fe} and v_{Fe} do not vary as the flow changes direction (presumably due to changes in the field direction). In the case shown in Figure 4, this proportionality is easily seen because of the large excursions in the east-west angle. Furthermore, if we use the measured values for V_{He}, v_{He} and ϕ_{He} in our model, we reproduce the measured 10/9 ratio both qualitatively and quantitatively. While deviations in ϕ_{He} and ϕ_{Fe} of this magnitude are rare, the nearly one-to-one correspondence between ϕ_{He} and log (10/9) is commonly observed. Thus all the observations and the results of the modeling imply that the parameters V, v, and ϕ are very

close to being identical in value for the minor ions He and Fe. This is consistent with our findings in Paper 2, and allows us to generalize those results from the specific cases cited there to most of the high speed streams (V_{He} > 600 km s^{-1}) for the period 1972-1976.

LONG TERM TRENDS

Returning to the repeatability of the corotating stream associated Fe/H ratios, we exploit this feature in Figure 5 by averaging five consecutive solar rotations of data in mid-1974 to obtain a more continuous, representative longitude record of Fe/H than a single rotation with its attendant data gaps (due to the magnetospheric passes of the spacecraft) can provide. The stream on the right is fairly constant in Fe/H at a level lower by a factor of ~ 2 than the stream shown in Figure 2. The stream from 0° to 170° has a longitude-dependent Fe/H ratio, decreasing from a value a factor of ~ 2 above the stream centered at 260° to a value perhaps a factor of 3 below that value, for a total change of a factor of ~ 6 from one edge of the stream to the other. The stream between 0° and 170° is associated with the equatorward extension of the south polar coronal hole. As shown by Mitchell et al. (1981b) for Carrington Rotation 1610, this hole was centered at the equator near 120°, but east of that longitude its equatorward edge sloped gradually to more and more southerly latitudes as the longitude decreased to ~ 30°. In Mitchell et al. (1981b), that structure was suggested as the source of latitudinal structure observed in that stream using multiple spacecraft measurements. We suggest here that the same topology may be related to the systematic decrease in Fe/H from west to east in this stream, in which the south-easterly orientation of the eastern boundary of the coronal hole allows us to sample the composition across the edge (which is not possible for the

more usual meridional orientation). If this is the case, the implication is that Fe/H is higher for solar wind originating near the inner edges of the coronal hole boundary region, decreasing as one approaches the outer edge of the boundary region. Whether or not the above can be stated in general, we believe the highly repeatable structure in the 0° - 170° Fe/H ratio is the signature of a long term stable coronal structure which modulates either the substrate Fe/H level, or the acceleration of Fe into the solar wind, or both.

We have taken this process of summing over multiple rotations one step further. By summing over an entire year, and then taking estimates by eye of the minimum, maximum, and mean Fe/H values for each year, we can examine (Figure 6) the yearly trend in Fe/H over the four years 1973-1976 during the decline of sunspot Cycle 20. It is clear that there is a monotonic decrease in Fe/H over the period. There is also a decline in He/H over the same period (upper curve, data from Feldman et al., 1978), but the iron abundance decrease precedes the helium abundance decrease by at least a year. The difference between the trends in Fe/H and He/H is actually greater than Figure 9 portrays, since the iron data is all from high speed streams while the downturn in He/H is dominated by the low speed solar wind; in fact, Bame et al. (1977) reported that He/H at the higher speeds remained remarkably constant (~ 5%) over this same period in the maxima of high speed streams. Thus, we find that the iron and helium abundances in high speed streams differ in their behavior on both intermediate (one stream's duration) and long term (fraction of a year to fraction of a solar cycle duration) time periods, though they are sometimes well correlated on a fraction of a daytime scale.

Some caution should be exercised in interpreting this four-year trend in Fe/H. Our capability for measuring Fe/H did not come about by

design; it resulted from a serendipitous combination of the electronic threshold and aluminum coating of the silicon solid state detector. We do not know what possible long-term degradation in iron response the flight detectors may have incurred, especially considering that they are counting iron at efficiencies between 1% and 10%, and small changes in the detector dead-layer might affect the absolute detector iron response substantially. However, no obvious detector degradation has been detected in analyzing energetic proton data and one can see from Figure 6 that IMP-7 and IMP-8 independently measure the same changes in relative abundance. Consequently, we believe at present that the trend in Fe/H is most likely a true change in composition during 1972-79. We hope to test the stability of the response to iron by observing a return to the abundance levels for iron typical of the 1973-1976 period, in high speed streams during the decline of Solar Cycle 21 which we are only now entering.

SUMMARY AND CONCLUSIONS

Using the 50 - 200 keV ion channel of a solid state detector on the EPE experiment, we have obtained the only thermal iron measurements at solar wind speeds over 600 km s^{-1} during the decline of Solar Cycle 20, when the solar wind structure was dominated by stable corotating coronal hole associated high speed streams. We have found that:

1) The response of the EPE to Fe, when compared to the LANL He measurements is consistent with the iron bulk velocity, thermal velocity, and bulk flow angle being the same (on average) as those for helium.

2) We often see correlated behavior in the ratios Fe/H and He/H over fractions of days, but not over longer time periods.

3) The profile of Fe/H as a function of time or coronal source longitude is a stable, repeatable feature of a stable corotating high speed stream.

4) Fe/H within a corotating stream can vary significantly as a function of the plasma's coronal source longitude, up to a factor of ~ 6, and we have tentatively identified the edges of coronal holes with lower Fe/H than the centers.

5) Flare-associated increases, up to a factor of ~ 5 in Fe/H are observed.

6) A long-term decrease of a factor of ~ 4 is measured in Fe/H from 1973 to 1976 during the decline of solar cycle 20.

ACKNOWLEDGEMENTS

We wish to thank D. J. Williams for the use of the IMP-7 and 8 EPE data, and R. D. Zwickl for his assistance with the LANL plasma data. Our effort was supported in part by NASA through Grant NAGW 264.

REFERENCES

Asbridge, J. R., S. J. Bame, W. C. Feldman and M. D. Montgomery, Helium and hydrogen velocity differences in the solar wind, J. Geophys. Res., 81, 2719, 1976.

Bame, S. J., J. R. Asbridge, W. C. Feldman, and J. T. Gosling, Evidence for a structure-free state at high solar wind speeds, J. Geophys. Res., 82, 1487, 1977.

Bame, S. J., J. R. Asbridge, W. C. Feldman, E. E. Fenimore, and J. T. Gosling, Solar wind heavy ions from flare-heated coronal plasma, Solar Phys., 62, 179, 1979.

Bame, S. J., Solar wind heavy ions from energetic coronal events, in Solar Wind 4, edited by H. Rosenbauer, Rep. MPAE-W-100-81-31, p. 434, Max-Planck-Institut-für Aeronomie, Lindau, FRG, 1981.

Bochsler, P. and J. Geiss, Cross- and auto-correlations of speeds and kinetic temperatures of minor ions in the solar wind, EOS, Trans. AGU, 63, 424, 1982.

Dusenberry, P. B. and J. V. Hollweg, Ion cyclotron heating and acceleration of solar wind minor ions, J.Geophys. Res., 86, 153, 1981.

Feldman, W. C., J. R. Asbridge, S. J. Bame and J. T. Gosling, Long term variations of selected solar wind properties: IMP 6, 7 and 8 results, J. Geophys. Res., 83, 2177, 1978.

Geiss, J. and P. Bochsler, On the abundance of rare ions in the solar wind, in Solar Wind 4, edited by H. Rosenbauer, Rep. MPAE-W-100-81-31, p. 403, Max-Planck-Institut-für Aeronomie, Lindau, FRG, 1981.

Hirshberg, J., J. R. Asbridge and D. E. Robbins, The helium component of solar wind velocity streams, J. Geophys. Res., 79, 934, 1974.

Hollweg, J. V and J. M. Turner, Acceleration of solar wind He^{++}, 3, Effects of resonant and nonresonant interactions with transverse waves, J. Geophys. Res., 83, 97, 1978.

Hundhausen, A. J., An interplanetary view of coronal holes, in Coronal Holes and High Speed Wind Streams, edited by J. E. Zirker, p. 225, Colorado Associated University Press, Boulder, 1977.

Ipavich, F. M., A. B. Galvin, G. Gloeckler, D. Hovestadt, B. Klecker, and M. Scholer, Heavy ion charge states observed in the solar wind, Solar Wind 5, 1983.

Isenberg, P. A. and J. V. Hollweg, Finite amplitude Alfvên waves in a multi-ion plasma: propagation, acceleration, and heating, J. Geophys. Res., 87, 5023, 1982.

Marsch, E., K.-H. Mühlhäuser, H. Rosenbauer, R. Schwenn and F. M. Neubauer, Solar wind helium ions: Observations of the Helios solar probes between 0.3 and 1 AU, J. Geophys. Res., 87, 35, 1982a.

Marsch, E., C. K. Goertz and K. Richter, Wave heating and acceleration of solar wind ions by cyclotron resonance, J. Geophys. Res., 87, 5030, 1982b.

Mitchell, D. G. and E. C. Roelof, Thermal iron ions in high speed solar wind streams: Detection by the IMP 7/8 energetic particles experiments, Geophys. Res. Lett., 7, 661, 1980.

Mitchell, D. G., E. C. Roelof, W. C. Feldman, S. J. Bame and D. J. Williams, Thermal iron ions in high speed solar wind streams, 2. Temperatures and bulk velocities, Geophys.Res. Lett., 8, 827, 1981a.

Mitchell, D. G., E. C. Roelof and J. H. Wolfe, Latitude dependence of the solar wind velocity observed $\gtrsim$ 1 AU, J. Geophys. Res., 86, 165, 1981b.

Neugebauer, M., Observations of solar wind helium, Fundam. Cosmic Phys., 7, 131, 1981.

Nolte, J. T., A. S. Krieger, A. F. Timothy, R. E. Gold, E. C. Roelof, G. Viana, A. J. Lazarus, J. D. Sullivan, and P. S. McIntosh, Coronal holes as sources of solar wind, Solar Phys., 46, 303, 1976.

Ogilvie, K. W., Differences between the bulk speeds of hydrogen and helium in the solar wind, J. Geophys. Res., 80, 1335, 1975.

Ogilvie, K. W., Solar wind composition measurements - ISEE-3, EOS, 61, 1097, 1980.

Williams, D. J., The ion-electron magnetic separation and solid state detector detection system flown on IMP-7 and 8: $E_p > 50$ keV, $E_e > 30$ keV, NOAA Tech. Report ERL 393-SEL 40 (U. S. Dept. of Commerce), Oct. 1977.

Withbroe, G. L., The chemical composition of the photosphere and corona, The Menzel Symposium on Solar Physics, Atomic Spectra, and Gaseous Nebulae, ed. K. B. Gebbie, National Bureau of Standards Special Publication 353, 127, 1971.

FIGURE CAPTIONS

FIGURE 1 (a) Scatter plot of the logarithm of the EPE L1 detector iron response (5.5 minute averages) normalized by the LANL hydrogen flux, versus the LANL hydrogen velocity for all $V_H > 500$ km s^{-1} during 1973. (b) Scatter plot of the logarithm of the EPE L1 detector iron response normalized by the LANL helium flux, versus the LANL helium velocity. Note the reduced scatter above $V_{He} \sim 660$ km s^{-1}.

FIGURE 2 One-hour averages of IMP-7 LANL solar wind parameters and the EPE iron abundance for a coronal hole-associated high velocity stream, days 50 - 62, 1973. The top panel shows V_H (solid line) and V_{He} (dots). Second panel is the logarithm of the measured iron abundance (Fe/H) normalized by a coronal value of 4.7×10^{-5}. Third panel is the parallel and perpendicular thermal velocity for H, connected by a vertical bar, and the He thermal velocity (dots) displaced downward by 25 km s^{-1} so it is not obscured by the H data. Bottom panel is Log (N_H) (solid line), and Log (He/H) (dots) on a separate scale (right-hand margin).

FIGURE 3 Same stream as Figure 2 (light lines and dots), plus its recurrence on the following rotation (heavy lines and dots) plotted as a function of heliographic source longitude, assuming constant radial flow from the corona to 1 AU. Fe/H does not change over a solar rotation in this stream.

FIGURE 4 Flare-associated stream from days 116 to 123, 1973. The iron abundance reaches unusually high values in association with the flare activity. In the bottom panel, Log (Sector 10/Sector 9) for the EPE is shown to closely mimic the He east-west flow angle.

FIGURE 5 Average of velocities and Fe/H over 5 solar rotations in 1974, plotted versus source longitude. The stream from 225° to 300° shows fairly constant Fe/H, while the stream from 45° to 135° shows a roughly monotonic increase in Fe/H from east to west. This repeatable feature is associated with the morphology of the boundary of the coronal hole source region for this stream.

FIGURE 6 Four-year decrease in Fe/H during the decline of Solar Cycle 20. The decrease in He/H is dominated by low speed solar wind, while He/H was nearly constant (~ 5%) at high speeds, so the Fe/H and He/H trends are distinctly different in the peaks of HSS.

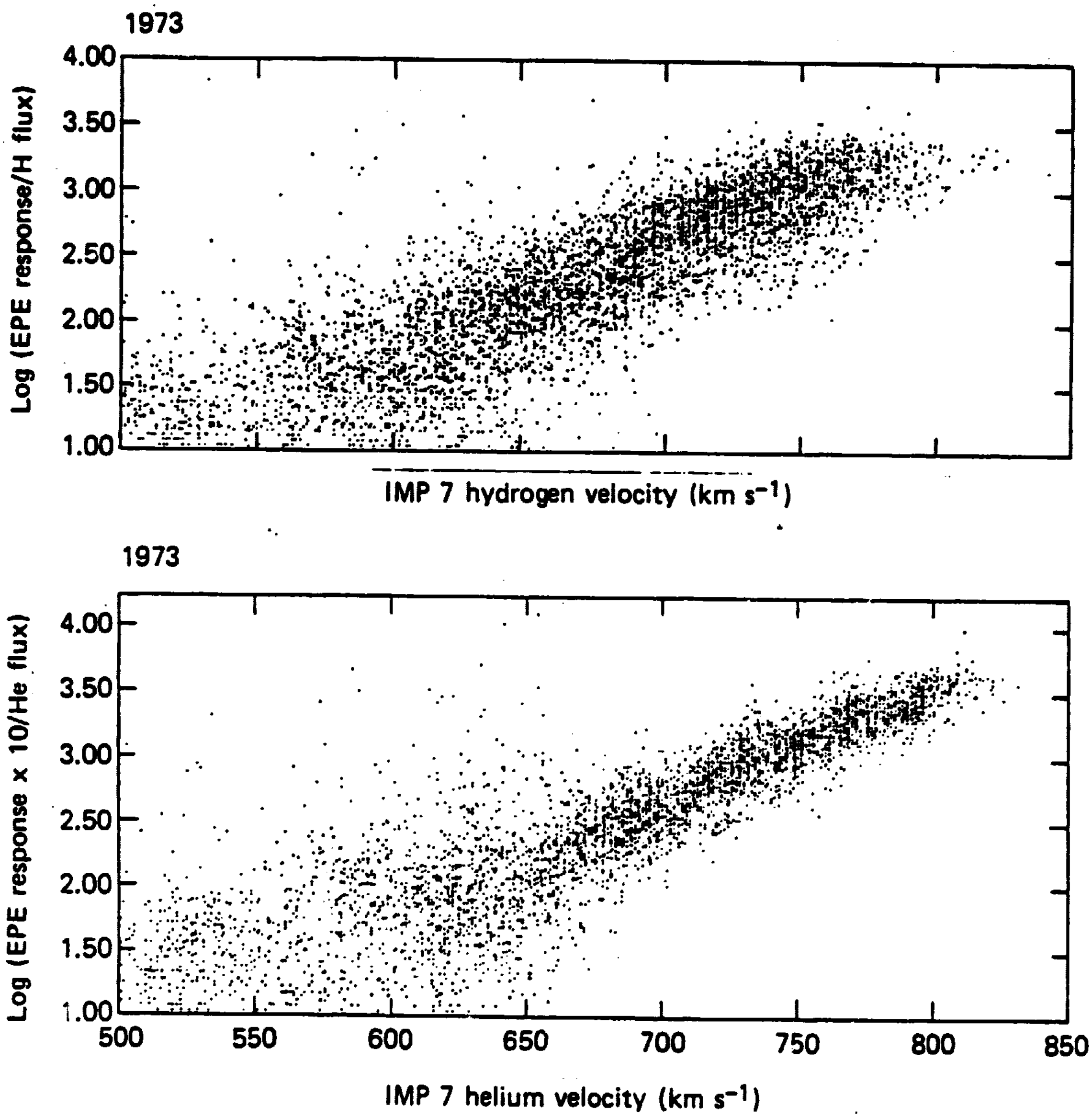
1973
Log (EPE response/H flux)
4.00
3.50
3.00
2.50
2.00
1.50
1.00
IMP 7 hydrogen velocity (km s-1)
1973
Log (EPE response x 10/He flux)
4.00
3.50
3.00
2.50
2.00
1.50
1.00
500
550
600
650
700
750
800
850
IMP 7 helium velocity (km s-1)

Figure 1

IMP-7

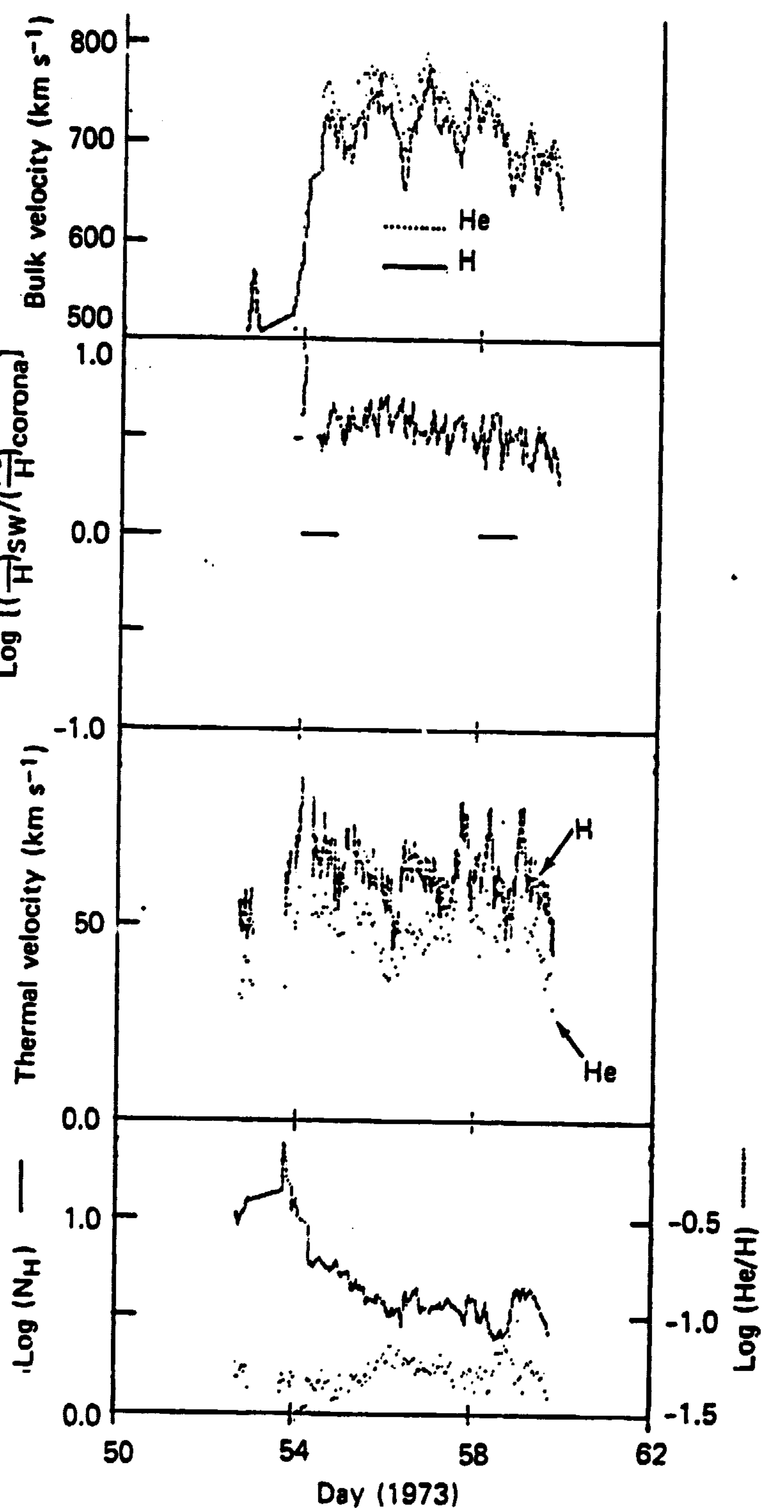

Figure 2

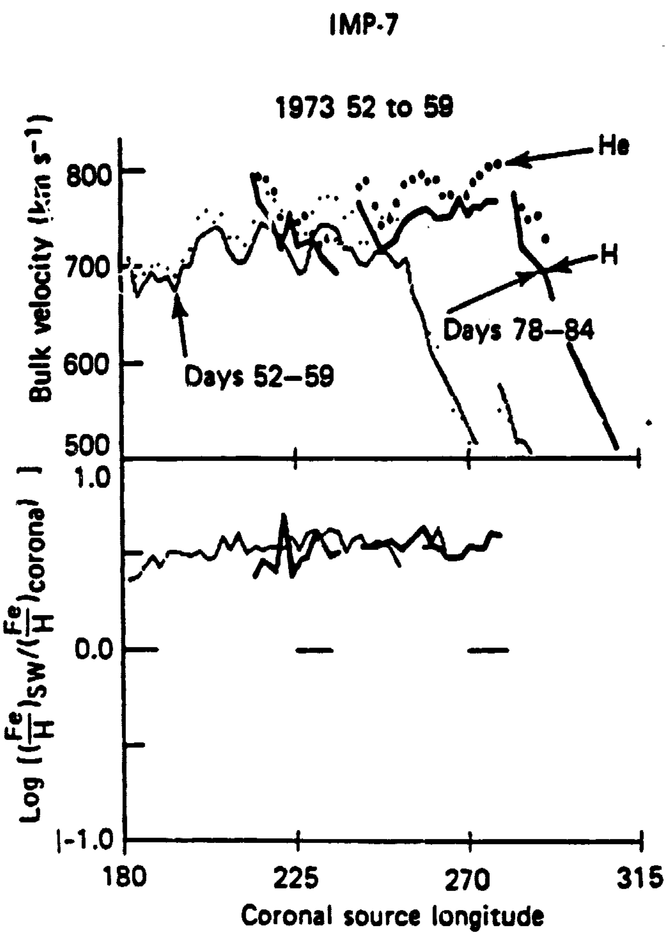
IMP-7
1973 52 to 59
Bulk velocity (km s^-1)
800
700
600
500
He
H
Days 52–59
Days 78–84
1.0
0.0
|-1.0
Log [(Fe/H)SW/(Fe/H)corona]
180
225
270
315
Coronal source longitude

Figure 3

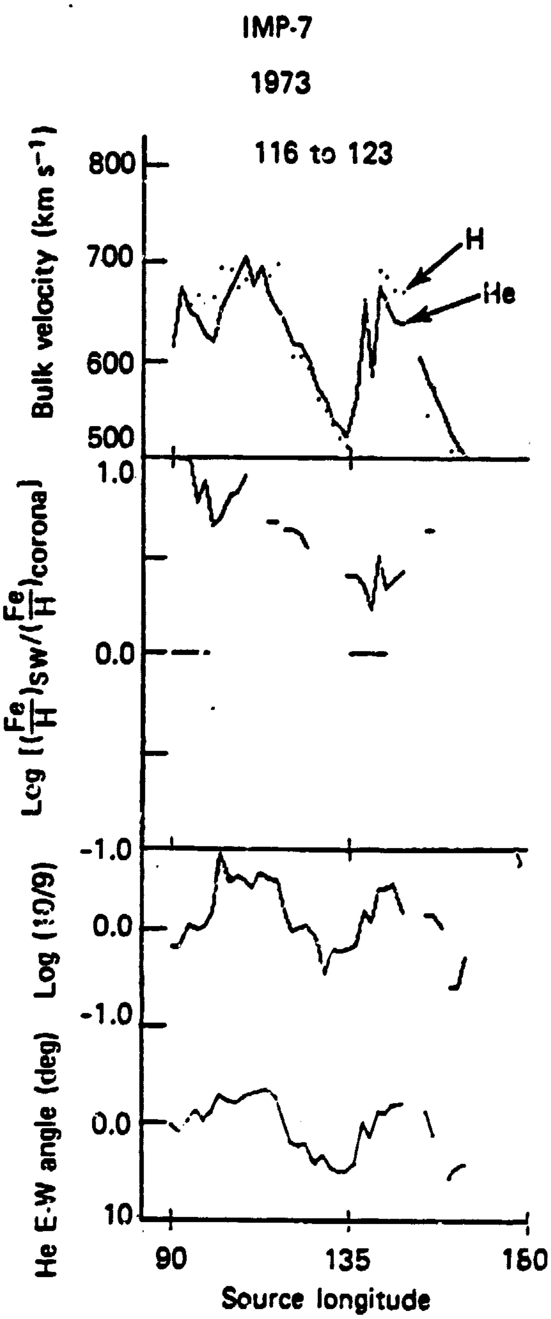
IMP-7
1973
116 to 123
Bulk velocity (km s^{-1})
800
700
600
500
H
He
Log [($\frac{Fe}{H}$)SW/($\frac{Fe}{H}$)corona]
1.0
0.0
-1.0
Log (10/9)
0.0
-1.0
He E-W angle (deg)
0.0
10
90
135
180
Source longitude

Figure 4

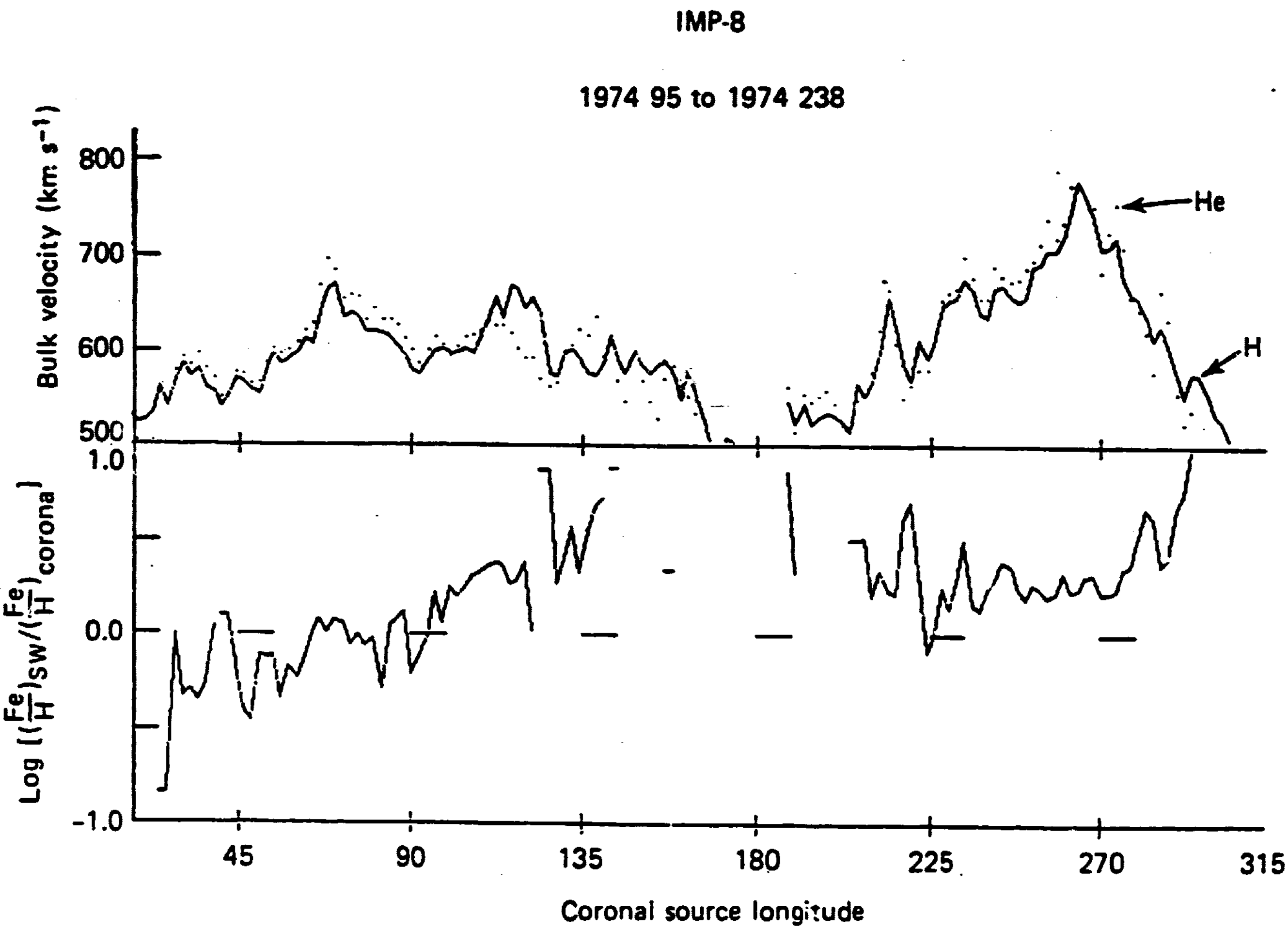

IMP-8
1974 95 to 1974 238
Bulk velocity (km s^{-1})
800
700
600
500
He
H
1.0
0.0
-1.0
Log [($\frac{Fe}{H}$)$_{SW}$/($\frac{Fe}{H}$)$_{corona}$]
45
90
135
180
225
270
315
Coronal source longitude

Figure 5

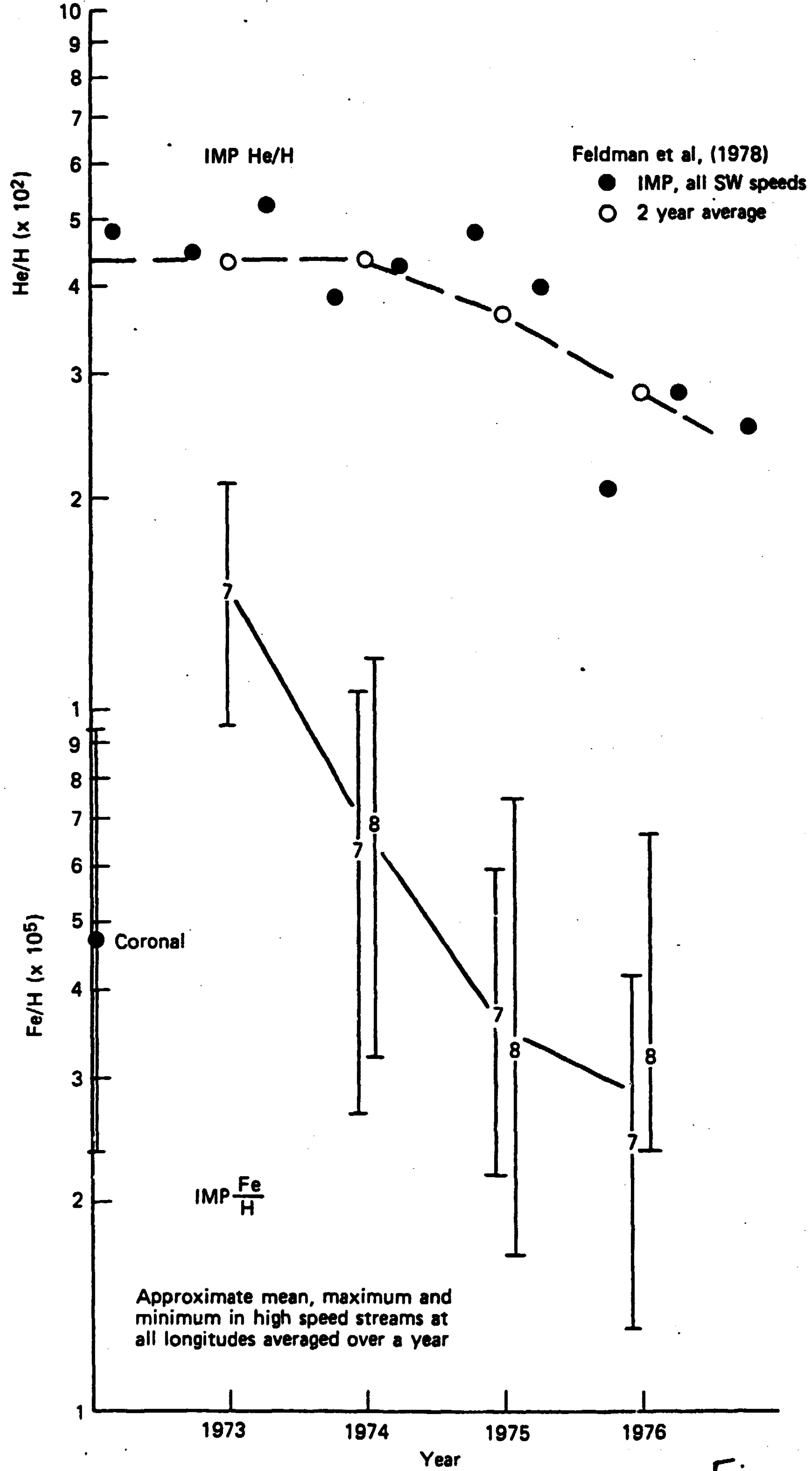

IMP He/H
Feldman et al, (1978)
IMP, all SW speeds
2 year average
He/H (x 10^2)
Fe/H (x 10^5)
Coronal
IMP $\frac{Fe}{H}$
Approximate mean, maximum and minimum in high speed streams at all longitudes averaged over a year
1973
1974
1975
1976
Year

Figure 6